JET-P(95)04

Fast Nonlinear Magnetic Reconnection

M Ottaviani, F Porcelli.

JET Joint Undertaking, Abingdon, Oxfordshire, OX14 3EA, UK.

Preprint of a paper to be submitted for publication in
Physics of Plasmas

February 1995

Abstract

The nonlinear evolution of magnetic reconnection in collisionless and weakly collisional regimes is analyzed on the basis of a two-dimensional incompressible fluid model. The initial equilibria are unstable to tearing modes. In the limit where the stability parameter Δ' is relatively large, the mode structure is characterized by global convective cells. It is found that the system exhibits a quasi-explosive time behavior in the early nonlinear stage where the fluid displacement is larger than the inertial skin depth but smaller than the typical size of the convective cells. The reconnection time is an order of magnitude shorter than the Sweet-Parker time for values of the inertial skin depth, of the ion Larmor radius and of the magnetic Reynolds number typical of the core of magnetic fusion experiments. The reconnection process is accompanied by the formation of a current density sub-layer narrower than the skin depth. In the strict dissipationless limit, this sublayer shrinks indefinitely in time. Physical mechanisms limiting this tendency to a singular current density profile are also discussed.

P.A.C.S. 52.35.Py

I. INTRODUCTION.

Laboratory plasmas close to thermonuclear conditions exhibit a variety of relaxation phenomena involving strong magnetic activity. The oldest known and best studied of these phenomena are sawtooth relaxations[1]. A common feature of these phenomena is the fact that they become more marked in the largest, hottest devices like the Joint European Torus (JET). In JET, for example, the ratio of the sawtooth period to the crash timescale exceeds three orders of magnitude. This is not unexpected on general grounds, since the crash time and the slow evolution should depend on different powers of the relevant Reynolds number (the magnetic Reynolds number).

Renewed interest in the crash problem was prompted by the observation[2] that at the high plasma temperatures of these experiments sawteeth can occur on a time scale shorter than the electron-ion collision time (see Fig. 1). Since the sawtooth phenomenon is associated with the m=1 internal kink, these experimental findings have generated considerable interest in the problem of magnetic reconnection in collisionless regimes, where electron inertia is responsible for the decoupling of the plasma motion from that of the magnetic field. In Astrophysics, of course, magnetic reconnection in collisionless regimes is thought to occur in several systems, such as for instance the low density environment of the Earth magnetosphere (see, e.g. the review article by Vasyliunas[3]).

Recently, the linear theory of m=1 kink-tearing modes has been extended to experimentally relevant regimes for plasmas close to thermonuclear conditions[4-7]. For the parameters of JET high temperature plasmas, the ion Larmor radius is larger than the plasma skin depth (examples are discussed at the end of Section III below). Under these conditions, magnetic reconnection in the linear stage can occur at a rate, normalized to the characteristic Alfven time, which is determined by an appropriate combination of the inertial skin depth and of the ion Larmor radius, normalized to the macroscopic size of the reconnection region, rather than by

collisional effects. This rate is significantly faster than that of the well-known resistive internal kink mode evaluated for the same plasma parameters. Thus, the conclusions from linear theory is that these modes can remain virulent at low collisionality with an initial growth rate which compares favorably with that observed in the experiments.

As usual, the validity of the linear theory is limited by the condition that the magnetic island width does not exceed the width of the reconnecting layer, in practice the electron skin depth, $d_e = c/\omega_{pe}$, or the ion Larmor radius, $\rho_i = (m_i c^2 T_i / e^2 B^2)^{1/2}$, whichever is larger. On the other hand, the example of Fig. 1 shows that the magnetic axis can move as fast as exponentially for a good fraction of the plasma size, well into the nonlinear stage.

The analysis of the nonlinear stage of fast sawtooth reconnection was initiated by Wesson[8]. Neglecting Larmor radius and pressure gradient effects, Wesson assumed that the nonlinear collisionless evolution qualitatively follows the standard Sweet-Parker[9-10] reconnection process in resistive MHD, but with the electron inertia replacing the collisional resistivity as the effective impedance to the electric field. Let us introduce a dimensionless reconnection time, τ_{rec}, measured in units of the characteristic Alfven time, the inverse magnetic Reynolds number, η, proportional to the electrical resistivity resulting from electron-ion collisions, and the dimensionless skin depth parameter $d \equiv d_e / a$, where a is a macroscopic scale length. Wesson suggested that the reconnection time shortens, going from the Sweet-Parker value $\tau_{rec} \sim \eta^{-1/2}$ when $d < \eta^{1/2}$, to the new value $\tau_{rec} \sim d^{-1}$ when $d > \eta^{1/2}$. This result can be interpreted as a consequence of the wider reconnection channel when electron inertial effects are considered. The channel width is $\delta_{rec} \sim \eta^{1/2}$ according to Sweet-Parker theory, but as the temperature is raised the relevant width cannot drop below the value $\delta_{rec} \sim d$. Interestingly, this nonlinear width is of the same order as the width found in the linear approximation (when Larmor radius effects are neglected). Similarly, Wesson's reconnection time turns out to be of the same order as the linear growth time. This led to the suggestion

that, in regimes where $\rho_i > d_e$, such that the ion Larmor radius sets the linear as well as the nonlinear width of the reconnection layer, the displacement may continue to grow exponentially well into the nonlinear phase [11], with a characteristic reconnection time $\tau_{rec} \sim a / \rho_i$.

Wesson's conclusions were questioned by Drake and Kleva [12], who simulated the merging of two isolated flux bundles. In this simulation, a new scale-length much smaller than the inertial skin depth was observed to develop during the nonlinear evolution. Using an argument from Sweet-Parker theory, namely that the reconnection time is proportional to the inverse width of the reconnection layer, and assuming that the relevant width corresponds to the newly found scale-length, Drake and Kleva concluded that the reconnection process would slow-down considerably as the nonlinear phase is entered, i.e. for magnetic island widths comparable with the plasma skin depth. This latter result would at least imply that the model studied cannot even qualitatively account for the experimental findings. This has induced some authors to investigate the behavior of more general models[11,13-14].

In this paper, first we discuss in detail the numerical and analytic solution of a reduced 2-D incompressible fluid model which neglects ion Larmor radius and pressure effects, essentially the model studied in Ref.[15] where preliminary results were reported. We find that, in the appropriate nonlinear regime, the current is mainly distributed over a distance d from the reconnecting surface, with a narrow inner sublayer shrinking with time. The physics of this narrow scale-length is qualitatively extraneous to Sweet-Parker theory. Indeed, as a consequence of the formation of the narrow sublayer, the reconnection process is found to exhibit a quasi-explosive behavior, in contrast with Drake&Kleva's conclusion. However, it is reasonable to expect that some physical process intervene at some stage during the nonlinear evolution, limiting the tendency to a singular current density profile.

Next, we turn our attention to dissipative effects, specifically to what extent they can limit the formation of this narrow current sub-layer. Of course, in a real

plasma, one can think of several collisionless mechanisms that introduce a spatial cut-off, such as, for instance, velocity space instabilities or 3-D effects. From our analysis it is tempting to conclude that, even in the presence of such limiting mechanisms, and as long as they do not affect the broader structure of the current channel, reconnection in weakly collisional regimes should proceed at least as fast as predicted by Wesson. However, more work is needed to validate this statement.

The possibility of magnetic reconnection in dissipationless regimes may raise questions of principle. It may be argued that the process is reversible and that the reconnection process may bounce back nonlinearly. One of the aims of the present paper is to clarify these aspects of the theory.

This paper is organized as follows. In Sec. II we present the model equations. The linear theory is discussed in Sec. III. General properties of the collisionless model, and in particular the question of reversibility, are discussed in Sec. IV. Sections V and VI report, respectively, the numerical and analytic solutions of the model equations in the collisionless limit. Numerical results with dissipation are discussed in Sec. VII. Our conclusions are presented in Sec. VIII.

II. MODEL EQUATIONS

We consider a two-dimensional model of magnetic reconnection, where the coordinate along the reconnection line is ignorable. A strong magnetic field is present along the direction of the ignorable coordinate. The perpendicular fluid motion is assumed to be incompressible, $\nabla \cdot \mathbf{v}_\perp = 0$, where $\mathbf{v}_\perp$ is the plasma flow in the plane orthogonal to the reconnection line. Ion Larmor radius effects are neglected in the bulk of the paper, thus the electrons and the ions move together at their $\mathbf{E} \times \mathbf{B}$ drift velocity in the perpendicular plane, $\mathbf{v}_{\perp e} = \mathbf{v}_{\perp i} \equiv \mathbf{v}_\perp$. Owing to their lighter mass, the parallel current density is carried mostly by the electrons, $\mathbf{J}_\parallel \approx -en_e \mathrm{v}_{\parallel e}$, while the parallel ion flow is neglected.

Our goal is to study the evolution of a reconnecting mode in the early nonlinear phase, defined by the condition $\delta_{linear} << \lambda << a$, where δ_{linear} is the width of the reconnection layer as given by linear theory, λ is the displacement of the magnetic axis and a is the macroscopic scale length. In this regime the behavior is expected to be universal, i.e. independent of the geometry. The model we consider is essentially an extension of reduced MHD on a slab, where the electron inertia terms, proportional to the square of the electron skin depth, $d_e^{\,2} \propto m_e$, are included in Ohm's law.

Therefore we consider the following equations:

$$\partial_t U + [\varphi, U] = [J, \psi], \tag{1}$$

$$\partial_t F + [\varphi, F] = \eta \nabla^2 (\psi - \psi_o) - \mu_e \nabla^4 \psi, \tag{2}$$

where we use the notation $\partial_t \equiv \partial/\partial t$ and $[A,B] \equiv \mathbf{e}_z \cdot \nabla A \times \nabla B$, with e_z the unit vector along the z direction. $U = \nabla^2 \varphi$ is the fluid vorticity, φ is the stream function, $\mathbf{v}_\perp = \mathbf{e}_z \times \nabla \varphi$ is the fluid velocity, $J = -\nabla^2 \psi$ is the current density along z, ψ is the magnetic flux function, $F \equiv \psi + d^2 J$, with d the normalized skin depth (skin depth parameter). Moreover, we have explicitly added some dissipative effects proportional to the electrical resistivity η and the electron viscosity μ_e.

The co-ordinate z is ignorable, $\partial_z = 0$. The co-ordinates x and y vary in the intervals $x \in [-L_x, L_x]$ and $y \in [-L_y, L_y]$, with the slab aspect ratio $\varepsilon \equiv L_x / L_y$. Periodic boundary conditions are imposed at the edge of these intervals. The magnetic field is $\mathbf{B} = B_o \mathbf{e}_z + \nabla \psi \times \mathbf{e}_z$, with B_o a constant value which we take to scale as $B_o \sim \varepsilon^{-1} |\nabla \psi|$ in order to mimic the magnetic field of a Tokamak. All quantities in Eqs. (1,2) are dimensionless, with L_x and $\tau_A = (4\pi \rho_m)^{1/2} L_x / B_y$ (the poloidal Alfven time) determining the length and time scale normalization. Thus the fields φ, U, ψ and J are normalized to $(B_o/c)(L_x^2/\tau_A)$, $1/\tau_A$, $L_x B_y$ and $(c/4\pi)(B_y/L_x)$, respectively.

Since the equations are normalized, the dissipation coefficients must be interpreted as the inverse of Reynolds-like numbers. Thus η is the ratio of the poloidal Alfven time to the resistive diffusion time and μ_e is the inverse of the usual electron Reynolds number based on the poloidal Alfven velocity.

This model can be extended to include ion Larmor radius effects[16-17] as well as ion diamagnetic frequency and electron pressure gradient effects. In regimes where the ion Larmor radius is large, a Pade approximation of the kinetic ion response allows a fluid-like modeling of the ion dynamics. We shall limit our discussion of these effects to the initial phase of the instability, where the main results from linear theory will be recalled. In the final discussion presented in Sec. VIII, it will be argued that the nonlinear evolution in regimes where electron pressure gradient effects become important may have to be treated with a full kinetic model for the electrons[17].

III. LINEAR STABILITY ANALYSIS

For typical plasma parameters, d, η and μ are small quantities. This enables the search for an analytic solution of the linear stability problem using standard asymptotic matching techniques. In particular, the electron inertia term and the resistive term have the structure of singular perturbations, which bring about topological transitions in the structure of the magnetic field.

When the small nonideal terms are neglected and stationary solutions satisfying $\partial_t = \varphi_0 = 0$ are considered, one finds that any periodic function $\psi(x) = \psi(x + 2L_x)$ is an acceptable equilibrium. We consider a simple equilibrium specified by $L_x = \pi$, $\varphi_o = U_o = 0$, $J_o = \psi_o = \cos x$, and $F_o = (1 + d^2)\psi_o$. This choice allows a completely analytic treatment of the linear problem. One finds that this equilibrium is tearing-unstable to linear perturbations of the type $(\varphi, \delta\psi) = \text{Real}\{[\varphi_L(x), \delta\psi_L(x)]e^{\gamma t + iky}\}$, where $\varphi_L(x)$ and $\delta\psi_L(x)$ are respectively odd and even functions around the two equivalent reconnecting surfaces at $x = 0$ and at $x = \pm L_x$. Instability occurs at long

wavelengths such that $k = m\varepsilon < 1$, where m is the mode number and ε the slab aspect ratio which must therefore be less than unity.

The linearized system of equations (1,2) can be written as

$$\gamma\left(\partial_x^2 - k^2\right)\varphi_L = (ik\sin x)\left(k^2 - 1 - \partial_x^2\right)\delta\psi_L \tag{3}$$

$$\gamma\left(1 - d^2\partial_x^2 + d^2k^2\right)\delta\psi_L + ik(1+d^2)\sin x\ \varphi_L = \eta(\partial_x^2 - k^2)\delta\psi_L \tag{4}$$

In the *outer* region, i.e. outside narrow layers around the reconnecting surfaces, the small terms proportional to γ, η and d^2 can be neglected. Thus, we obtain from (3) the single equation for $\delta\psi_L$,

$$\left\{\partial_x^2\delta\psi_L + (1-k^2)\delta\psi_L\right\}\sin x = 0 \tag{5}$$

while Eq. (4) yields the proportionality relation between φ_L and $\delta\psi_L$ in the outer region,

$$\varphi_L = \frac{i\gamma}{k\sin x}\delta\psi_L \tag{6}$$

Equation (5) allows a discontinuity in the first derivative of $\delta\psi_L$ across the two reconnection layers at $x = 0$ and $x = \pm L_x$, where $\sin x$ vanishes. If the two layers are equivalent, in the sense that the layer equations around $x = 0$ and $x = \pm L_x$ are identical, then we must choose the solution of Eq. (5) which has the same discontinuity across these layers (see below Eq. (16)). For $0 < k^2 \le 1$, this solution is

$$\delta\psi_L = \psi_\infty \cos\left[\kappa\left(|x| - \pi/2\right)\right] \tag{7}$$

with ψ_∞ a constant and $\kappa \equiv \left(1-k^2\right)^{1/2}$. The jump of the logarithmic derivative of $\delta\psi_L$ across the reconnecting layers is

$$\Delta' \equiv \left| \frac{d \ln \delta\psi_L}{dx} \right|_{x=0^-}^{x=0^+} = 2\kappa \tan\left(\frac{\kappa\pi}{2}\right). \tag{8}$$

Δ' in Eq. (8) is a positive parameter. As is well known, $\Delta' > 0$ is a necessary condition for instability of reconnecting modes. For the considered model, this condition is also sufficient. When $k^2 \geq 1$, the outer solution changes character, from sinusoidal to exponential, and the corresponding Δ' becomes negative. Thus, instability is possible only when $0 < k^2 \leq 1$, which requires values of the aspect ratio parameter $\varepsilon < 1$, as anticipated. When $0.5 \leq \varepsilon < 1$, only the mode with $m=1$ is unstable. The smaller ε, the larger the number of unstable modes, up the maximum mode number $m_{\max} = \text{integer}(\varepsilon^{-1})$.

In the *inner* region (inside the reconnection layers), we can approximate $\sin x \approx x$ and neglect small terms such as k^2 compared to ∂_x^2. Thus we obtain the equations

$$\gamma^2 \xi'' = -k^2 x \delta\psi'' \tag{9}$$

$$\delta\psi = x\xi + (d^2 + \eta/\gamma)\delta\psi'' \tag{10}$$

where we have introduced the linear *displacement* $\xi \equiv v_{xL}/\gamma = -(ik/\gamma)\varphi_L$, with v_{xL} the x-component of the perturbed velocity field. It is clear from these equations that, in the linear approximation, the only change introduced by electron inertia is in the constant coefficient multiplying $\delta\psi''$ in Eq. (10), where the resistive term η/γ is replaced by the combination $\Delta^2 \equiv (d^2 + \eta/\gamma)$. Noting that the magnetic Reynolds' number can be written as $\eta = d^2 \nu_{ei}/2$, where ν_{ei} is the electron-ion collision frequency normalized to the Alfven time, the parameter Δ can be written as

$\Delta = \left(1 + \nu_{ei}/2\gamma\right)^{1/2} d$, which shows that in the linear instability phase electron inertia prevails over resistivity for modes growing over a time scale shorter than the collisional time.

A solution of the inner equations can be conveniently found in (generalized) Fourier space, where the transformed displacement $\hat{\xi}(\zeta) = \int_{-\infty}^{+\infty} \xi(x) e^{-i\zeta x} dx$ satisfies the equation

$$\frac{d}{d\zeta}\left[\frac{\zeta^2}{1+(\Delta\zeta)^2}\frac{d\xi}{d\zeta}\right] - \hat{\gamma}^2\zeta^2\xi = 0 \tag{11}$$

where $\hat{\gamma} \equiv \gamma / k$. This equation must be solved subject to the asymptotic boundary conditions

$$\xi(\zeta) \sim \text{const}\left[\zeta^{-1} + (\pi/\Delta')\,\text{sign}(\zeta) + \mathcal{O}(\zeta)\right], \text{ for } \zeta \to 0, \tag{12}$$

$$\xi(\zeta) \to 0 \text{ for } |\zeta| \to \infty. \tag{13}$$

These conditions, which are appropriate only for positive values of Δ', ensure the proper matching of the inner and the outer solutions and determine the growth rate $\hat{\gamma}$ as an eigenvalue problem. For negative Δ', the outer solution changes character, as we already mentioned, and the boundary condition (12) has to be reconsidered.

The solution of (11-13) can be found in terms of Kummer's hypergeometric functions $U(a,b;z)$,

$$\xi(\zeta) = \text{const}\cdot\exp\left(-\delta_L{}^2\zeta^2/2\right)\Xi(\zeta) \tag{14}$$

$$\Xi(z) = U\left(\frac{Q+1}{4}, \frac{3}{2}; z\right) - \frac{1}{2} z U\left(\frac{Q+5}{4}, \frac{5}{2}; z\right) \tag{15}$$

where $\delta_L \equiv (\hat{\gamma}\Delta)^{1/2}$ is a measure of the linear layer width and $Q \equiv \hat{\gamma}/\Delta$. The eigenvalue condition is

$$\hat{\gamma} = -\frac{\pi}{\Delta'}\left(\frac{Q}{4}\right)^{3/2}\frac{\Gamma[(Q-1)/4]}{\Gamma[(Q+5)/4]} \qquad (\Delta' > 0) \tag{16}$$

Since we are dealing with two layers, we point out that in the general case where the parameter Q may have different values at the two layers, the proper matching procedure yielding a unique solution for the eigenfrequency $\hat{\gamma}$ requires a specific ratio in the values of the outer Δ' parameter at the two layers. For two equivalent layers, this ratio must be taken equal to unity.

The dispersion relation (16) is well known. In particular, in the collisional limit[18-19], it yields the limiting expressions for the mode growth rate and layer width

$$\hat{\gamma} \sim \delta_L \sim \eta^{1/3} \quad \text{when} \quad \Delta'\eta^{1/3} >> 1, \quad d << \eta^{1/3} \tag{17}$$

$$\hat{\gamma} \sim \eta^{3/5}(\Delta')^{4/5}, \quad \delta_L \sim \eta^{2/5}(\Delta')^{1/5} \quad \text{when} \quad \Delta'\eta^{1/3} << 1, \quad d << \eta^{1/5}(\Delta')^{-2/5} \tag{18}$$

In the opposite limit of infrequent collisions, one finds the scalings[20-21]

$$\hat{\gamma} \sim \delta_L \sim d \quad \text{when} \quad \Delta' d >> 1, \quad d >> \eta^{1/3} \tag{19}$$

$$\hat{\gamma} \sim d^3(\Delta')^2, \quad \delta_L \sim d^2(\Delta')^1 \quad \text{when} \quad \Delta' d << 1, \quad d >> \eta^{1/5}(\Delta')^{-2/5} \tag{20}$$

Of particular interest is the change in the mode structure going from small to large positive values of Δ' (Fig. 2). In the limit $\Delta' d << 1$ (or $\Delta'\eta^{1/3} << 1$ in the collisional case) the mode structure corresponds to a standard tearing mode. In this case, $\delta\psi_L$ is nearly constant across the reconnection layers, while φ_L is localized

near these layers, that is to say the corresponding flow cells have a characteristic width $L_{cell} \sim \delta_L$. In the opposite limit of large Δ', i.e. $\Delta' d >> 1$ (or $\Delta' \eta^{1/3} >> 1$), $\delta\psi_L$ varies rapidly across the reconnection layers, while the structure of the stream function is macroscopic, with $\varphi_L \approx \varphi_\infty \operatorname{sign} x$, $\varphi_\infty \equiv (i\gamma/k)\psi_\infty$, everywhere except in the reconnection layers. The profiles of the current density and of the stream function in the vicinity of the layer at $x=0$ take the form $\delta J_L \approx -\psi_\infty \left(2/\pi d^2\right)^{1/2} \exp\left(-x^2/2d^2\right)$ and $\varphi_L \approx \varphi_\infty \operatorname{erf}\left(x/2^{1/2} d\right)$, which match onto the outer solution for $|x| > d$. Thus we can say that the large Δ' regime is characterized by macroscopic flow cells with $L_{cell} \sim L_x >> \delta_L$.

This distinction between large and small Δ' regimes is essential in the following discussion of the nonlinear mode evolution. In the small Δ' regime we expect a very slow nonlinear growth of the magnetic island on the resistive time scale, as described by Rutherford[22]. The large Δ' regime allows an intermediate nonlinear phase[15], characterized by magnetic island widths satisfying the inequalities

$$\delta_L < w_{isl} < L_{cell} \tag{21}$$

We shall show that fast nonlinear magnetic reconnection can take place during this intermediate nonlinear phase.

Extensions of linear theory

The discussion above already indicates that the linear growth rate of the reconnecting mode does not decrease with increasing temperature as a purely collisional model would predict, but that it saturates to a value determined by the inertial skin depth according to the simple model discussed above. In reality, as the temperature becomes higher and higher, it is no longer possible to neglect finite ion Larmor radius effects. If we separate between nonlocal (kinetic) effects and

diamagnetic frequency effects associated with gradients in the equilibrium pressure, both of which are brought in by the finite Larmor radius, we can show that the former effects cause a *further enhancement*[4,23] of the linear growth rate, while the latter effects exert a stabilizing influence, introducing a large-Δ' threshold for the excitation of reconnecting modes[4,24]. It can be argued that, once this threshold is crossed and the magnetic island reaches a width of the order of the ion Larmor radius, diamagnetic effects are quenched and the mode grows according to the large Δ' regime discussed in the following sections.

The discussion of ion Larmor radius effects has already been presented in the literature. Thus we limit ourselves to recall briefly the main results.

The additional scalelengths occurring in finite temperature theory are the proper ion Larmor radius ρ_i and the ion *sound* Larmor radius, $\rho_s = c_s / \Omega_{ci}$, where $c_s = (T_e / m_i)^{1/2}$ and $\Omega_{ci} = eB / m_i c$. For realistic plasma parameters, the *proper* ion Larmor radius effects and the ion sound Larmor radius effects should be considered simultaneously, since $\rho_s / \rho_i = (T_e / T_i)^{1/2} \sim 1$. Early investigations[25,26] of reconnecting modes in collisionless regimes considered the cold-ion limit, $\rho_i \to 0$, while retaining effects associated with finite ρ_s. The cold ion approximation implies that a fluid model for the ions can be assumed, while a full kinetic treatment for the electrons was employed in the mentioned early investigations. In this case the linear width of the collisionless current channel is determined by the inertial skin depth (although the stream function varies rapidly over a distance of order ρ_s), so that the fluid ion approximation remains valid as long as $\rho_i < d_e$. Now,

$$(\rho_i / d_e) = (m_i \beta_i / 2m_e)^{1/2} \tag{22}$$

tends to be larger than unity for values of the ion $\beta_i = 8\pi p_i / B^2$ parameter that are of interest in controlled thermonuclear experiments. Therefore, the analysis of Porcelli[4] was aimed at extending the early analyses to the regime where $\rho_i > d_e$. This extension requires a full kinetic (Vlasov) treatment of the ion dynamics,

leading to a rather involved integro-differential dispersion equation in coordinate space (see, e.g., Ref.[27]). The analysis simplifies in Fourier space, where an ordinary differential dispersion equation can be obtained. This simplification arises provided ion Landau damping can be neglected. This, however, is a safe approximation in so far as modes are found whose complex frequency satisfies $\omega >> k_{\|} v_{thi}$, where $k_{\|} \sim \delta_L / L_y$ is the parallel wavelength. As for the electrons, a fluid approximation can be assumed, with the generalized Ohm law

$$\mathbf{E} + \frac{1}{c}\mathbf{V}_e \times \mathbf{B} = \eta \mathbf{J} + \frac{m_e}{n_e e^2}\left(\frac{\partial}{\partial t} + \mathbf{V}_e \times \nabla\right)\mathbf{J} - \frac{1}{n_e e}\nabla \cdot \tilde{\mathbf{P}}_e \tag{23}$$

where $\tilde{\mathbf{P}}_e$ is the electron pressure tensor and the other terms have their usual meaning. The fluid electron model requires a closure. In the large ρ_s or ρ_i limits, it can be shown *a posteriori* that this closure is accomplished by the choice of an isothermal equation of state. Of course, the fluid electron approximation excludes the treatment of modes whose growth or damping may depend on Landau resonant processes.

A great analytic simplification is obtained by adopting a Pade' approximation of the kinetic ion response, as discussed in Ref. [16,23] . With this approximation, the two scale lengths ρ_s and ρ_i combine into a single scale length equal to their geometric mean,

$$\rho_\tau = (\rho_i^2 + \rho_s^2)^{1/2} = (1+\tau)^{1/2}\rho_i \ , \tag{24}$$

where $\tau \equiv T_e / T_i$. The implication is that a result correct in the ion kinetic regime can be recovered simply replacing ρ_s by ρ_τ in the dispersion relation obtained earlier in Refs. [25-26]. A similar conclusion was reached by Aydemir[28], who employed a four-field model to analyze the stability of $m=1$ modes, and by Zakharov and Rogers[7], who used the two-fluid Braginskii model. We point out,

however, that the stream function is significantly different in the cold and kinetic ion regimes[29], as is shown below. In addition, the Pade' approximation is not entirely correct if temperature gradient effects are included in the ion response function. Then, only the kinetic description can fully account for the proper ion equation of state[23].

The dispersion relation in the limit $\hat{\rho} \equiv \rho_s / a > d$, $\hat{\gamma} < \hat{\rho}$ and $\eta = 0$ is

$$(\pi/2)\hat{\gamma}^2 = -\pi\hat{\rho}/\Delta' + \hat{\rho}^2 d/\hat{\gamma} \tag{25}$$

(for a derivation see Ref.[4]). In the limit $\Delta' \to \infty$, we obtain the growth rate

$$\hat{\gamma} \approx (2/\pi)^{1/3} d^{1/3} \hat{\rho}^{2/3} \equiv \hat{\gamma}_0 \tag{26}$$

which is higher than the growth rate in Eq. (19) by a factor $(\hat{\rho}/d)^{2/3}$. A modest enhancement of this growth rate, by a factor $(1+\hat{\nu}_{ei}/2\hat{\gamma})^{1/6}$, is found for $\nu_{ei} \le \gamma_0$.

For $(\hat{\rho}d^2)^{1/3} < \lambda_H < \hat{\rho}$, where $\lambda_H = -\pi/\Delta'$ is the stability parameter of cylindrical geometry, the growth rate $\hat{\gamma} \sim (\lambda_H \hat{\rho})^{1/2}$ is obtained from (25). The ideal MHD result, $\hat{\gamma} \sim \lambda_H$, applies to the limit $\lambda_H > \hat{\rho}$, where Eq. (25) is no longer valid. In the limit $\Delta' < (\hat{\rho}d^2)^{-1/3}$, Eq. (25) yields $\hat{\gamma} \sim \hat{\rho} d\Delta'$, so that for small Δ' the growth drops below the collision frequency and the (semi)collisional regime is recovered. A graph of $\hat{\gamma}/\hat{\gamma}_0$ versus the parameter $\lambda_H/(\rho^{1/3}d^{2/3})$ is shown in Fig.3.

Examples of the perturbed parallel current density and of the electrostatic potential across the reconnection layer for $\Delta' \to \infty$ and $\hat{\rho}_s/d = 5$ are shown in Fig.4. The larger part of $J_\parallel(x)$ is localized over a distance $x \sim (\hat{\rho}/d)^{1/3} d$, where the decoupling of the electrons from the magnetic field lines can occur, with a tail extending up to distances $x \sim \rho_s$. This profile remains unchanged in the cold ion limit $T_i \to 0$ keeping ρ_s fixed $(T_e \to 2T_e)$. On the other hand, the profile of the stream function is very different in the cold and kinetic ion limits. For kinetic ions $(T_i \sim T_e)$, $\varphi(x)$ varies rapidly up to distances $x \sim d$, while it approaches a constant

over distances $x \sim \rho_\tau$. This behavior reflects the decoupling of the electron and ion radial flows at distances $x < \rho_i$. By contrast, for fluid ions ($T_i / T_e \to 0$), the structure around $x \sim d$ disappears and $\varphi(x)$ varies gently over the scale length ρ_s.

These considerations bring about the question of the validity of the assumed isothermal equation of state for the electrons. As we have seen, the current density is localized over a distance $x \sim (\hat{\rho}/d)^{1/3} d \equiv \delta_J$. It can be easily checked that this is also the distance where $\hat{\gamma}_o^2 \sim k_\parallel^2 v_{the}^2$. Below this distance, the isothermal approximation for the electrons breaks down. On the other hand, the eigenvalue condition is determined by asymptotic matching in the interval $\delta_J < x < \hat{\rho}$. Thus a correct result for the eigenfrequency to leading order in the small parameter $d/\hat{\rho}$ is obtained when an isothermal equation of state is chosen across the entire layer. This conclusion is supported by the numerical analyses of Refs.[5-6], who investigated the linear stability properties using a kinetic electron model which more properly represents the electron equation of state.

These results are valid as long as diamagnetic effects can be neglected. These effects have been considered by Porcelli[4] following the earlier analysis of semi-collisional $m=1$ modes by Pegoraro et al.[23]. The main findings are as follows. Using a Pade' approximant for the kinetic ion response function, the modified dispersion relation at ideal MHD marginal stability ($\Delta' \to \infty$) is

$$(\gamma + i\omega_{*e})(\gamma + i\omega_{*i})^{2/3}(\gamma + i\omega_{di})^{1/3} = \gamma_0^2 \tag{27}$$

where $\omega_{*e} = (cT_e / eBr_s)(d\ln n_e / d\ln r)_s$, r_s is the radius of the reconnecting surface in a toroidal plasma (the $q=1$ surface for the case of the sawtooth instability), $\tau\omega_{*i} = -\omega_{*e}$, $\omega_{di} = (1+\eta_i)\omega_{*i}$ and $\eta_i = d\ln T_i / d\ln n_i$. Then, assuming $\tau \sim 1$, stabilization is predicted when

$$\frac{\omega_{*i}}{\gamma_0} = \frac{1}{2}\left(\frac{\pi}{1+\tau}\right)^{1/3}\left(\frac{m_i}{m_e}\right)^{1/6}\left(\frac{L_s}{r_n}\right)\beta_i^{2/3} > 1 \tag{28}$$

For finite values of Δ' we may conclude that a threshold exists, $\Delta' = \Delta'_{cr}(\omega_*)$, corresponding to the criterion $\hat{\gamma}(\Delta', \omega_*) = \omega_*$, with $\hat{\gamma}(\Delta', \omega_*)$ the solution of the dispersion relation (25). The threshold (28) is found to correlate very well with the onset and stabilization of sawteeth in recent Tokamak Fusion Test Reactor (TFTR) supershot discharges[30]. It should be pointed out that the Pade' approximant for the kinetic ion response is not entirely correct when $\hat{\gamma} \sim \omega_*$ and η_i becomes large. For instance, using the full kinetic ion response, a residual growth rate for values of $\eta_i > \eta_{i,crit} \approx 1.6$ was found in Ref. 23.

The main conclusion of the linear analysis is that magnetic reconnection in the large Δ' regime can remain a very fast process at high temperatures, contrary to expectations based on collisional models. In Fig. 5 we present a sketch of γ versus $T \equiv T_e = T_i$ for near ideal MHD marginal stability conditions ($\Delta' \to \infty$), keeping all other parameters constant. At low temperatures, the resistive growth rate scales as $\gamma \sim T^{-1/2}$. At intermediate temperatures, corresponding to $(\hat{\rho}/\eta^{1/3})^{2/7} d < \eta^{1/3} < \hat{\rho}$, one finds the semi-collisional growth rate $\gamma \approx (2/\pi)^{2/7} \hat{\rho}^{4/7} \eta^{1/7} \propto T^{1/14}$, which is virtually independent of the temperature. At higher temperatures, the collisionless growth rate (26) increases with temperature as $\gamma \propto T^{1/3}$. In this regime the condition for diamagnetic stabilization for $\Delta' \to \infty$ involves the plasma beta parameter [cf. Eq. (28)]. This condition is more stringent than predicted by the two-fluid resistive model. The stabilization condition $\omega_* > \gamma$ is more easily met for values of $\Delta' < -\hat{\rho}^{-1/3} d^{-2/3}$, where γ drops below γ_0.

Let us now evaluate the relevant stability parameters for internal kink modes in JET high temperature discharges. We choose the reference values $R = 3m$, $B = 3T$, $n_e = 3. \times 10^{19} m^{-3}$ and $T_e = 5keV$ near the $q = 1$ surface. With the effective charge $Z_{eff} = 2$, the electron-ion collision time is $\tau_{ei} \approx 130 \mu s$. Thus $\nu_{ei} \approx \tau_{ei}^{-1}$ is 1 to 4 times smaller than the experimental growth rate of Fig. 1. The plasma skin depth is $d_e \approx 1mm$. Considering a deuterium plasma with $T_i \approx T_e$, the ion gyroradius is $\rho_i \approx 1/3cm$. Assuming a parabolic q profile with $q_o = 0.7$ and a $q = 1$ radius

$r_s = 0.3m$ we find $\gamma_o^{-1} \approx 70\mu s$. Thus γ_o^{-1} agrees within a factor 2 with the observed growth time. Finally $\beta_e(r_s) \approx 0.6\%$ and assuming a density scale length $L_n \approx 1m$ we have $\omega_{*_e} / \gamma_o \approx 0.36$.

IV. GENERAL PROPERTIES OF THE NONLINEAR COLLISIONLESS MODEL.

In this section we discuss some properties of Eqs. (1-2) in the inviscid (dissipationless) case.

We start by noting that Ohm's law can be interpreted as a conservation law for the quantity F. F is simply advected by the flow, which means that the value of F on a given fluid element is conserved. Upon restoring the physical dimensions, one finds that $F \propto m_e \mathrm{v}_z - e\psi / c$, where v_z is the velocity of the electron fluid in the z direction. Thus F is proportional to the density of the electron toroidal canonical momentum at a given point. Since the fields do not depend on z, the *particle* canonical momentum along z is always conserved. One cannot however conclude that the conservation of F on the fluid element is a general property of the two-dimensional models. One must also impose the condition that the electrons move together with the fluid (i.e., the ions) in the (x,y) plane, as in the derivation of Eqs. (1-2).

Note that in general, the electron guiding center drift in the (x,y) plane is given by:

$$\mathbf{v}^e = \frac{c}{B}\mathbf{E}\times\mathbf{B} + \mathrm{v}_z \frac{\mathbf{B}_\perp}{B} \tag{29}$$

where $\mathbf{B}_\perp$ is the magnetic field in the (x,y) plane. On the other hand the fluid is subject only to the $\mathbf{E}\times\mathbf{B}$ motion. Thus the fluid canonical momentum is conserved only when the projection on the (x,y) plane of the electron drift along

the field lines (the second term in the r.h.s. of Eq. (29)) can be neglected. This condition turns out to be $v_z\psi / c\varphi << 1$. Upon using ideal MHD with $\omega \approx k_{\parallel} v_A$ one obtains $v_z / v_A << 1$. For thermal electrons this condition becomes $\rho_s / d_e << 1$, as expected from the range of validity of Ohm's law in the form given in Eq.(2).

The pointwise conservation of F brings about the existence of two families of integral invariants:

$$I_1 = \int dxdy f(F) \tag{30a}$$

and

$$I_2 = \int dxdy U g(F) \tag{30b}$$

where $f(F)$ and $g(F)$ are arbitrary functions. In addition the total energy is also conserved:

$$E = \tfrac{1}{2} \int dxdy [(\nabla\varphi)^2 + (\nabla\psi)^2 + d^2(\nabla^2\psi)^2] \tag{30c}$$

We now use the conservation of F to show that a singularity should form. Consider a hyperbolic stagnation point of the flow (X-point). Such points are for example the X- and the O-points of the isolines of ψ when the initial conditions for Eqs. (1-2) are the linear eigenfunctions. Assuming x to be the direction of the stable manifold one can approximate the equation of the fluid element as $dx/dt = -v_0(t)x/d$. Then the fluid elements converge exponentially to the X-point according to $x = x_0 e^{-\lambda/d}$, $\lambda(t) = \int_0^t v_0(\tau)d\tau$. If F has nonzero derivatives along x, these derivatives are exponentially amplified. Moreover, if F is analytic in the complex x-plane in a strip containing the x axis, the width of the strip will shrink exponentially. Thus the occurrence of a singularity at $t = +\infty$ is generic and does not occur only when the system evolves to a state of zero flow (a new equilibrium).

The formation of a singularity in F brings about a related current sheet around the X-point of the flux function. The nature of this singularity is discussed more in detail in the next sections.

We now present a more general heuristic argument as why singularities are expected in the evolution of fields satisfying equations like Eqs.(1-2) in the dissipationless case. Assume smooth initial conditions. The existence of derivatives of arbitrary order implies that the Fourier spectrum must decay at least exponentially at large wavenumbers. This means that although the spectrum will usually have a power law range, this would extend up to a maximum wavenumber, say k_M, where the exponential portion of the spectrum begins. Naturally k_M will change with time as the fields evolve. Three possibilities can in principle occur, as sketched in Fig. 6.

1) $k_M(t)$ stays bounded as $t \to +\infty$.

2) $k_M(t)$ grows indefinitely as $t \to +\infty$. The solution exists at all the times but the spectrum spreads as times goes on.

3) $k_M(t)$ becomes infinite at some finite time t_c. Then the field becomes singular and the solution ceases to exist.

We argue that the first option is not possible for *generic initial conditions*. Assume for the moment that $k_M(t)$ stays bounded. Then, upon truncating the equations to some wavenumber $k_U >> k_M$ one can replace the continuum system with a finite number of Fourier modes, at the price of introducing an exponentially small error. However it is known that such a system will *in general* evolve into a spectrum whose time average is a power-law all the way to k_U (see Ref.[31]). The exact form of the spectrum depends on the invariants of the system and on the value of these invariants. For a truncated system the invariants are of the form given in Eqs. (30a-c) when only *quadratic* terms are retained. Thus the probability distribution is a Gibbs distribution of the form $P[\varphi,\psi] \propto \exp(-\alpha I_1 - \beta I_2 - \gamma E)$,

where α, β, and γ are Lagrange multipliers. When computing the expectation value of the Fourier components of the fields, one concludes that the spectra are rational functions of the wavenumbers. This contradicts the assumption that the spectrum decays exponentially for $k > k_M$.

The third option is also unlikely to occur. Indeed a consequence of the existence of pointwise invariants like the vorticity has been used to show that the solution of the two-dimensional Euler equation remains C^∞ for all the times when the initial conditions are C^∞[32]. Although no proof is known for Eqs.(1-2) it is commonly thought that 2-d fluid equations possessing topologic invariants have the same properties. In Eqs.(1-2) the quantity F is such an invariant. (Although we have used F to show that a singularity is expected, the very existence of this invariant makes the singularity milder).

Thus one concludes that a singularity will in general occur but only at $t = +\infty$.

Finally we comment on the issue of reversibility. Clearly Eqs. (1-2) are reversible. It is therefore interesting to pose the question of principle whether the reconnection taking place in this system is only a transient phenomenon and the magnetic field will eventually unreconnect[33].

One can see that this would be the case if one assumes that the system goes into a saturated state with zero flow. Indeed zero flow states have the property that F and ψ are functionally dependent, $F = f(\psi)$, which implies that F and ψ possess the same set of isolines. Since the topology of F has not changed, the topology of ψ in the final state would be the same as in the initial state, although the final configuration could be different.

Essential to this argument is the assumption that the system goes back to rest as $t \to +\infty$. However it is unlikely that this would happen. A generic trajectory of a multidimensional system (actually an infinite dimensional system) is nonperiodic. Even when the system departs from the equilibrium at $t = -\infty$ along the unstable manifold, there are no reasons why it should come back to the same equilibrium (or to another equilibrium) at $t = +\infty$ along a stable manifold. We simply do not expect

that the system comes back to rest or that follows a periodic trajectory. Only in this latter case would the initial magnetic field topology be restored. In this sense one could qualify the reconnection process as *irreversible.*

In practice, irreversibility (in the usual meaning) is anyway introduced by the effect of dissipation, which comes into place when the microscale becomes small enough, as discussed in a later section.

V. NUMERICAL RESULTS IN THE DISSIPATIONLESS CASE.

The numerical investigation of Eqs. (1,2) has been carried out with a pseudospectral code[34] which advances in time the Fourier representation of the field variables, truncated to 1024×64 (x,y) components.

In the choice of the slab aspect ratio we are motivated by conflicting requirement. On the one hand, in analogy with the internal kink, we are interested the *large-*Δ' regime, which can be achieved for low values of m and $\varepsilon^2 << 1$ such that $\Delta' \sim (8/\pi k^2)$ can be made arbitrarily large. On the other hand we want just one mode (m=1) to become unstable. This sets a lower bound on the aspect ratio $\varepsilon = 1/2$, hence an upper bound on $\Delta' \approx 8.12$. Most of our studies were carried out with $d = 1/4$, thus satisfying the large Δ' condition as well as allowing a good scale separation ($d/2L_x = 0.04$).

The initial conditions are chosen to approximate closely the linear eigenfunctions of the unstable model with small amplitudes. The initial conditions are such that the X-points of these islands are $x = 0$, $y = 0$ and $x = L_x$, $y = L_y$. The spatial symmetries of the initial conditions, namely reflection symmetries with respect to the reconnection line and with respect to the four points $x = \pm L_x/2$, $y = \pm L_y/2$ are preserved during the nonlinear evolution.

The results of a collisionless simulation ($\mu_e = \eta = 0$) are summarized in Figs. 7-10.

Fig. 7 shows sections of $\delta\psi \equiv \psi - \psi_o$, $v_x = -\partial\varphi / \partial y$, J and F across the X-point $(y = 0)$ at various times. $\delta\psi$ and v_x are normalized to their value at $x = -L_x/2$. Initially the systems evolves essentially linearly. This phase lasts conventionally until $t \sim 80$, when the magnetic island reaches a width of order d. Until this time, the profiles shown in Figs. 7a,b are very close to the linear eigenfunctions. The linear layer width $\delta_{\text{linear}} \sim d$ is visible from these graphs.

For $t > 80$, the system behaves nonlinearly. Note that the width of the profiles of $\delta\psi$ and v_x remains of the order of the skin depth (Figs. 7a,b). By contrast, the current density profile and the invariant F (Fig. 7c-d) develop a time dependent scalelength which keeps shrinking with time, in agreement with the analysis of Sec. IV. This behavior is confirmed in Fig. 8d, which shows the evolution of the inverse of the scalelengths of v_x and J, measured, respectively, by $\delta_\varphi \equiv (v_x)_{x=L_x/2} / (\partial_x v_x)_{x=0}$ and $\delta_J \equiv \left(\partial_x^2 \delta J / \delta J\right)^{-1/2}$ (Here, $\delta J \equiv J - J_o$). One can see that δ_φ is little changed while δ_J becomes rapidly small.

Figs. 8a-c show profiles of $\delta\psi$, $\partial_x^2 F$ and v_y versus y along the reconnection line, at various times. Note in particular the X-point/O-point asymmetry developed by the flux function (Fig. 8a). The curvature of the profile of F, $\partial^2 F / \partial x^2$, grows around the X-point and decreases around the O-point as a consequence of the conservation property combined with the flow direction (Fig. 8b). At $t \approx 125$, the nonlinear microscale has become so narrow that it can no longer be resolved by our truncated Fourier expansion, and so the simulation is stopped. By contrast, the profile of the y component of the velocity (Fig. 8c) does not change much from the linear phase.

Contour plots of φ, ψ, J and F are shown in Fig. 9. Note again that the convection cells retain approximately their linear shape well into the nonlinear phase (Fig. 9a). The same is apparent for the magnetic island (Fig. 9b). Also note the development of a current sheet around the reconnection line (Fig. 9c) and the preservation of the topology of the isolines of F (Fig. 9d).

Finally, the time behavior is illustrated in Fig. 10. It is remarkable that the mode growth remains very rapid throughout the simulation. Indeed, the growth of φ, as well as that of $\delta\psi$ and δJ at the X-points, accelerate in the early nonlinear phase, which suggests that the growth is quasi-explosive.

To summarize this section, we have found that the reconnection rate in the purely collisionless case accelerates nonlinearly. The electric potential and the flux function maintain a "broad" structure, with a characteristic scalelength nowhere smaller than the electron skin depth. Conversely, the current (and the vorticity) develop a nonlinear time dependent microscale which decreases with time. In the next section we will show how the above findings are coherently explained with analytic calculations.

VI. ANALYTIC APPROACH.

The conservation of F allows the formal integration of the collisionless Ohm's law (2):

$$F(x,y,t) = F_o[x_o(x,y,t)] = (1+d^2)\cos[x_o(x,y,t)] \ , \tag{31}$$

where $x_o(x,\, y,\, t) = x - \xi(x,\, y,\, t)$ is the initial position of a fluid element situated at (x,y) at time t and ξ is the displacement along the x direction defined by the equation $d\xi/dt = \mathrm{v}_x$, $\xi(t=-\infty) = 0$.

As discussed in the previous section, the numerical results suggest that the spatial structure of the stream function does not vary significantly with time throughout the linear and early nonlinear phases. This motivates the ansatz:

$$\varphi(x,\, y,\, t) = \mathrm{v}_o(t)g(x)h(y) + u(x,y,t) \ , \tag{32}$$

where $h(y) \sim k^{-1}\sin(ky)$, $g(x) \sim \varphi_L(x)/\varphi_\infty$ contains the linear scale length d and $u(x,y,t)$ develops the rapid scale length $\delta(t) \sim \delta_J$ observed in the numerical simulation. We assume $u << \mathrm{v}_o$ and $\partial_x u \sim \mathrm{v}_o \partial_x g$, which is consistent with the near constancy in time of the width of v_x across the reconnecting layer (Fig. 8d), as well as that of the ratio $\mathrm{v}_y\left(0, L_y/2, t\right)/\mathrm{v}_x\left(-L_x/2, 0, t\right)$ (Fig. 10). This assumption allows a parametrization of the system of Eqs. (1,2) in terms of the displacement $\lambda(t) = \int_0^t \mathrm{v}_o(\tau)d\tau$.

By integrating the equation of the fluid element along the line $y = 0$ (across the X-point), $dx/dt = \mathrm{v}_x$, and neglecting the contribution from $u(x,y,t)$, one gets

$$-\int_{x_o}^{x} dx'/g(x') = \int_{-\infty}^{t} \mathrm{v}_o(t')dt' \equiv \lambda(t). \tag{33}$$

In the large Δ' regime, the leading behavior can be extracted by approximating $g(x)$ as $g(x) = x/d$ for $|x| < d$ and $g(x) = \pm 1$ for $|x| > d$. Inverting Eq. (32) one gets the dominant contribution to the function $x_o(x, y, t)$ in three characteristic spatial ranges bounded by the linear scale d and by the nonlinear microscale

$$\delta(t) \equiv d\exp\left[-\lambda(t)/d\right] \quad :$$

$$x_o \sim x(d/\delta) \qquad \text{for } |x| < \delta \tag{34a}$$

$$x_o \sim d\ln\left(e|x|/\delta\right)\mathrm{sign}(x) \qquad \text{for } d > |x| > \delta \tag{34b}$$

$$x_o \sim \lambda\,\mathrm{sign}(x) + x \qquad \text{for } |x| > d \tag{34c}$$

Analogous relations are obtained along the $ky = \pi$ line, crossing the O-point, by swapping x and x_o.

A sketch of the dependence of x_o on x is presented in Fig. 11. Thus we see that near the X-point along the x direction, $F(x_o)$ (and hence J) varies over a distance $\delta(t)$ which becomes exponentially small in the ratio λ/d. Conversely, around the O-point $F(x_o)$ flattens over a distance $|x| \sim \lambda$ from the O-point, as observed numerically.

The flux function can be expressed in terms of F by means of the proper Green's function. Here we neglect the derivatives along y, which is justified in the large Δ' limit. Moreover we replace the Green's function defined in the box with the one defined in the plane. This is a valid approximation in the range of interest $x < \lambda << L_x$:

$$\psi(x,y,t) \approx \tfrac{1}{2d}\int_{-\infty}^{\infty} e^{-|x-x'|/d} F(x',y,t)dx', \tag{35}$$

One can see that any fine scale variation of F is smoothed out over a distance of order d. Therefore d is the smallest scalelength of the leading contribution to ψ. Asymptotic evaluation of the deviation from the equilibrium $\delta\psi$ and δJ can be derived from Eq. (35) by using Eq. (31) and Eqs. (34). Along the line $y = 0$ crossing the X-point we find:

$$\delta\psi = -\tfrac{1}{2}\lambda^2 + \mathcal{O}(\lambda d) \qquad \text{for } x < d \tag{36a}$$

$$\delta\psi = -\tfrac{1}{2}\lambda^2 - \lambda x + \mathcal{O}(d^2) \qquad \text{for } d < x << L_x \tag{36b}$$

and:

$$\delta J = -\tfrac{1}{2}\lambda^2 / d^2 \qquad \text{for } x < \delta \tag{37a}$$

$$\delta J \approx -(\lambda/d)\ln(x/d) - \tfrac{1}{2}[1+\ln(x/d)]^2 + \mathcal{O}(\lambda/d) \qquad \text{for } \delta < x < d \tag{37b}$$

$$\delta J = \mathcal{O}(\lambda/d)\exp(-x/d) \approx 0 \qquad \text{for } x > d \tag{37c}$$

The logarithmic singularities in expressions for the current would have appeared as subdominant corrections to Eq. (36a).

We can see that the current perturbation is distributed over a region of width d. (At finite values of Δ', as in numerical experiment, there are delocalized corrections to Eq. (37c) which come from the y-derivative of $\delta\psi$. These are apparent in Fig. 7c).

The current density has a peak of order $\delta J_X \sim 0.5(\lambda/d)^2$ and an average value of order $\lambda/d >> 1$ (i.e., much bigger than the equilibrium current density) in the region $|x| < d$.

A similar calculation can be carried out along the line $y = L_y$, crossing the O-point. In the following, we will only need the values at the X- and O-points:

$$\delta\psi_X \sim -\tfrac{1}{2}\lambda^2(t), \quad \delta\psi_O = \mathcal{O}(d^2), \tag{38}$$

as well as the relation $\delta J = -\delta\psi/d^2$, valid along the reconnection line where $\delta F = 0$. Thus we have demonstrated that an asymmetry develops in the values of $\delta\psi$ and of δJ between the X- and O-points, as observed numerically (Fig. 8a).

Let us now integrate the vorticity equation (1) over the quadrant $S:\left[0 \le x \le L_x, 0 \le y \le L_y\right]$. Using Stokes theorem, we obtain

$$\partial_t \int_C \mathbf{v}\cdot d\mathbf{l} = \oint_C \omega d\varphi + \oint_C J d\psi = \oint_C J d\psi . \tag{39}$$

where C is the boundary of S, i.e. the quadrangle XO'X'O which connects the critical points of the two symmetric islands (Fig. 12). We have use the fact that $d\varphi = 0$ on C. By exploiting the symmetry with respect to $(L_x/2, L_y/2)$ one realizes that it is enough to integrate along the lines OX and XO'. As a rule the integrals along XO' gives only a subdominant contributions in the large Δ' limit.

The l.h.s. of Eq. (38) is dominated by the integral of v_y (the integral of v_x contributes to order $\mathcal{O}(\varepsilon kd)$). Using the ansatz (32), and neglecting corrections contributed by $\partial_y^2\varphi$, we find

$$\partial_t \int_C \mathbf{v}\cdot d\mathbf{l} \approx -\left(2c_0c_1/k^2d\right)d^2\lambda/dt^2 , \tag{40}$$

where $c_0 = d\left(dg/dx\right)_{x=0} = \mathcal{O}(1)$ and $c_1(t) = 1 + \left(d/c_0 v_o\right)\left(\partial_x u\right)_X$ is a factor of order unity, which depends weakly on time (e.g. $1 \le c_1 \le 1.4$ in Fig. 8d).

The r.h.s. of Eq. (38) can be written as

$$\oint_C J d\psi = -\int_0^{L_y} dy \left(J \partial_y \psi \right)_{x=0} - \int_0^{L_x} dx \left[(\partial_y^2 \psi)(\partial_x \psi) \right]_{y=0}.$$

The first integral at the right hand side can be evaluated exactly:

$$-\int_0^{L_y} dy \left(J \partial_y \psi \right)_{x=0} = \delta\psi_X - \delta\psi_O - \left(\delta\psi_X^2 - \delta\psi_O^2 \right) / 2d^2 \tag{41}$$

The second integral is bounded to $\mathcal{O}(k^2\lambda)$, which is subdominant both in the linear and in the nonlinear phase.

Using an interpolation formula between the linear and early nonlinear limits of the r.h.s. of (40), we obtain an equation for the evolution of $\hat{\lambda}(t) \equiv \lambda(t)/d$:

$$d^2\hat{\lambda}/d\hat{t}^2 \approx \hat{\lambda} + c_2\hat{\lambda}^4 \tag{42}$$

where $\hat{t} \equiv \gamma_L t$ and $c_2 \approx 1/16 c_0 c_1$ can be taken constant. The solution is $\hat{\lambda}(\hat{t}) = \left[(1-\alpha) / \left(1 - \alpha e^{3\hat{t}} \right) \right]^{2/3} e^{\hat{t}}$, where $\alpha = \beta - (\beta^2 - 1)^{1/2}$, $\beta = 1 + 5/c_2$, and we have chosen the time origin so that $\hat{\lambda}(0) \equiv 1$. Thus, once the early nonlinear regime is entered, $\lambda(t)$ accelerates and reaches a macroscopic size over a fraction $\sim \ln(\alpha^{-1/3})$ of the linear growth time. This explains the acceleration is clearly visible in Fig. 10. Detailed comparison of the prediction of Eq. (42) and the result of the numerical experiment is however made difficult by the resolution which limits $\hat{\lambda}$ to $\hat{\lambda} = \ln(d/\delta_{\min}) \approx 3.7$.

This explosive growth will eventually turn into a slower growth as λ approaches the macroscopic scale length. It is interesting to ask whether there is a bound on the growth of λ. In this model there is an overall bound to the maximum attainable velocity set by the energy conservation law (Eq. 30c). This means that, asymptotically, λ cannot grow faster than linearly in time. Note that in this range λ

would cease to be the displacement as it would grow bigger than the macroscopic length. In reality, new physics will come into play much earlier, as discussed later.

We conclude this section with a discussion of the consistency of the ansatz (32).

The surface integral that has led to Eq. (42) has allowed the annihilation of the vorticity nonlinearity. However, *pointwise*, the vorticity term is dominant in the nonlinear regime. In order to do show that this is the case, we estimate $u(x,y,t)$ directly from the equation of motion (Eq. 1) using the expressions of ψ and J obtained with the ansatz (32). We then show that the resulting expression for $u(x,y,t)$ satisfies the assumed ordering.

In the region $\delta < x < d$ the vorticity nonlinearity is approximated by $[\varphi_{\text{linear}}, \partial_x^2 u]$, since, by assumption, $[u, \partial_x^2 u]$ is subdominant. In a strip around the x-axis we can approximate $u(x,y,t) \approx w(x,t)y$. Upon using the piecewise expression for φ_{linear} introduced below Eq. (33), and the asymptotic expression $[J,\psi] \approx \partial_x(\delta J)\partial_y(\delta\psi) \sim -\lambda^3 y/(dx)$, which is valid in the nonlinear regime, one is led to an equation for w:

$$\partial_t \partial_x^2 w + (d\lambda/dt)(1/d)(\partial_x^2 w - x\partial_x^3 w) \approx -\lambda^3/(dx) \tag{43}$$

From Eq. (42) one gets $d\lambda/dt \approx \lambda^{5/2}/d^{1/2}$. The leading contribution to w is then

$$w \approx xd\ln(x/d)(\lambda/d)^{1/2}. \tag{44}$$

One can immediately verify that the ansatz (32) as well as the other assumptions that led to Eq. (44) are satisfied. In particular $\partial_x w/\partial_x\varphi_{\text{linear}} \leq (d/\lambda) << 1$ in the range $\delta < x < d$. Note also that $\partial_t w$ is subdominant in Eq. (43). Thus the vorticity nonlinearity *is a dominant term* of Eq. (1) in the reconnection region. Indeed the vorticity can diverges as $1/x$ for $x \to \delta$ without invalidating the ansatz.

VII. NUMERICAL RESULTS WITH DISSIPATION.

The nonlinear, time-dependent microscale $\delta(t)$ obtained in the previous sections becomes rapidly small. One therefore expects that it will be replaced by some cutoff when additional physics is taken into account. In this section we analyze how dissipation can modify the previous phenomenology. We will also discuss the question whether the evolution can proceed at a fast rate even in the presence of the additional physics. This is especially relevant in order to address the experimental findings.

We first discuss the role of resistivity. It is interesting, to compare the results of a family of simulations possessing the same linear behavior, but differing in the nonlinear stage. This is made possible by the fact that linear theory is unaffected by a change of the pair of values of (η,d) if the growth rate and the quantity $\eta+d^2\gamma$ are held constant, and initial conditions are the same.

A purely resistive case which matches the previously studied collisionless case corresponds to $\eta=3.\times10^{-3}$ when $d=0$. The nonlinear stage is however completely different from the collisionless case, as seen from Fig. 13. In particular the development of the current sheet proceeds in a much slower fashion. In the purely resistive case the system is expected to follow the Sweet-Parker behavior[9-10]. A detailed analysis of the pure resistive case is outside the scope of this work.

In contrast with the purely resistive case, a "balanced" case $(\eta=1.5\times10^{-3}, d=1/4\sqrt{2})$, when resistivity and electron inertia contribute *equally* to the linear phase, behaves essentially in a collisionless fashion (Fig. 14). This behavior is understood by inspecting Ohm's law (2) using the expressions for the flux function and for the current given by Eqs. (36-37). One can see that the resistive term in the spike region is bounded to $\mathcal{O}(\eta\lambda^2/d^2)$ which is smaller than the l.h.s. of Eq. (2) (which is $\mathcal{O}(\lambda d\lambda/dt)\geq\mathcal{O}(\gamma_{linear}\lambda^2)$) for small values of η. In other words the resistive term is a regular perturbation (the order of the differential

operator is too low) and does not introduce a small scale cut-off. This situation persists as long as $\eta < \gamma_{linear} d^2$, or $\eta^{1/3} < d$, which is also the condition to neglect resistivity in the linear theory. When this condition applies we speak of *collisionless regime.*

Consider now the effect of electron viscosity (one does not necessarily think of a true (collisional) viscosity at this point: any process acting as a current hyperdiffusivity would be equivalent). Inspection of Ohm's law reveals that the electron viscosity term is $\mathcal{O}[\mu_e(\lambda/d)(1/x^2)]$ at a distance x from the X-point. Thus, sufficiently close to it, any nonzero viscosity can balance the leading collisionless terms. The viscosity operator is a singular perturbation. This idea has been confirmed by running simulations with μ_e in the range $4.\times 10^{-7} \le \mu_e \le 6.4 \times 10^{-6}$. See Fig. 14.

When resistivity is large enough that $d < \eta^{1/3}$, it cannot be treated perturbatively. In the linear phase the electron inertia terms are negligible and the displacement grows with $\gamma_{linear} \approx \eta^{1/3}$ until the displacement it becomes of the order of the width of the linear layer $\lambda \approx \delta_{linear} \approx \eta^{1/3}$. A detailed numerical investigation of the nonlinear regimes would require simulations with small enough values of the resistivity, to discriminate between the various scaling laws. In our system, this is not possible without violating the large Δ' condition. Here we present our conjectures about the expected behavior in these regimes.

In the nonlinear stage the behavior initially follows the Sweet-Parker scenario with the layer width shrinking as $\delta_{nonlinear} \approx (\eta/\lambda)^{1/2}$ while the displacement grows as a power law $\lambda \approx \eta t^2$. If $d < \eta^{1/2}$ (*strong collisionality regime*) the displacement reaches the macroscopic size $\lambda \approx 1$ when $\delta_{nonlinear} \approx (\eta)^{1/2}$. In this case the reconnection proceeds in a purely resistive fashion on a timescale of the order of the characteristic Sweet-Parker-Kadomtsev[9,10,35] time $\tau_{SPK} \approx \eta^{-1/2} \approx (\tau_{Alfven}\tau_{Resistive})^{1/2}$.

When the skin depth falls in the intermediate range $\eta^{1/2} < d < \eta^{1/3}$ (*moderate collisionality*) a new regime occurs[36]. In this case the inertia terms become important when $\delta_{nonlinear} \approx d$. This occurs at some value of the displacement

$\lambda^* \approx \eta / d^2$ after a time $t^* \approx d^{-1}$. Afterwards we expect that the reconnection proceeds essentially in a collisionless fashion until $\lambda \approx 1$. The reconnection time is therefore controlled by the electron inertia, $\tau_{rec} \approx d^{-1} << \tau_{SPK}$, throughout the collisionless and the moderate collisionality regimes.

This behavior can be summarized by the phenomenological equation for $\hat{\xi} \equiv \lambda / \eta^{1/3}$:

$$\frac{d\hat{\xi}}{dt} = \left(\frac{1 + \hat{d}^2 \hat{\xi}}{1 + \hat{\xi}} \right)^{1/2} \hat{\xi} \tag{45}$$

where $\hat{t} = \eta^{1/3} t$ and $\hat{d} = d / \eta^{1/3}$. The numerical solution of Eq. (45) is shown in Fig. 15. The growth eventually saturates when the displacement reaches a macroscopic size, $\lambda \sim L_{cell}$.

The typical JET experiments shown in Fig. 1 belong to the borderline between the collisionless and moderate collisionality regimes: here the reconnection time turns out at least an order of magnitude shorter than the Sweet-Parker-Kadomtsev time: $\tau_{rec} / \tau_{SPK} \approx \eta^{1/6} < 10^{-1}$. This ratio is further reduced when Larmor radius effects are included.

VIII. DISCUSSION AND CONCLUSIONS.

The applicability of a fluid model to the study of collisionless magnetic reconnection will depend, of course, on the plasma parameters that one considers. It can be argued that a fluid model is appropriate as long as the instability has a non-oscillatory character, which excludes regimes where diamagnetic frequency effects are important. Then wave-particle effects are not significant and the bulk of the fluid is involved in the instability process. The problem is to identify the appropriate closure to the moment hierarchy.

When $\rho_i \sim \rho_s < d_e$ one can show that the adiabatic equation of state is the appropriate closure for both electrons and ions throughout the linear and nonlinear phases[4]. Pressure effects are never dominant in this regime and one can equivalently assume $p = 0$ to the leading order.

The *linear theory* in the opposite regime, $\rho_i \sim \rho_s > d_e$, is complicated by the presence of two nested layers around the reconnecting surface[4]. It can be shown that linear theory can be consistently developed within the fluid approximation using the isothermal equation of state for the electrons and a Pade approximation for the kinetic ion response . Strictly speaking the isothermal approximation breaks down inside the inner layer, $|x| < \delta_{in}$, but the eigenfunctions do not exhibit any significant structure over this distance[4].

The validity of fluid theory in the nonlinear regime when $\rho_i \sim \rho_s > d_e$ is more delicate. The point is that the development of a nonlinear scalelength $\delta(t) < \delta_{in}$ is expected on general grounds (Sec. IV). Thus no equation of state can be used uniformly in this regime, and a kinetic treatment, even in the absence of resonances seems unavoidable[17].

The nonlinear evolution of the dissipationless model (1,2) is characterized by a rapidly decreasing microscale. When the displacement has become few times the skin depth, this microscale has decreased to values comparable to the Debye length or to the electron Larmor radius. It is therefore relevant to ask what are the physical mechanisms which could slow down the process of the current spike formation. *More importantly, to understand the experimental findings, it is necessary to verify whether the fast growth of the displacement can be sustained even in the presence of spike cut-off mechanisms.*

As far as the actual cut-off mechanisms, we have discussed the possible role of dissipation in the previous section. It has been shown that a small amount of resistivity does not provide an effective cutoff, as the resistive diffusion operator is a *regular perturbation*. An effective cutoff may be introduced by electron viscosity or by a hyperresistivity term simulating the effect of magnetic microturbulence.

Other possibilities to be explored include instabilities of the current sheet[12]. Note that our calculation assumes a well defined parity in the initial conditions. When this constrained is relaxed, secondary instabilities of different parity can occur. Another possible current instability (not treatable within our model) is two-stream instability associated with the distortion of the electron velocity distribution function[8]. Finally we note that stochasticity associated with three-dimensional geometry can also be effective, especially since fast electrons are generated.

Concerning the question of whether the reconnection rate is affected by the spike cut-off mechanism, we first recall that the faster-than-exponential nonlinear stage is caused by a $\mathbf{J}\times\mathbf{B}$ nonlinearity associated with the X-point/O-point asymmetry. Since the current is distributed over the width of the linear layer δ_{lin}, this nonlinearity should be little affected by the presence of a cutoff which alters the current profile mainly in the inner region $x \leq \delta_{cutoff} << \delta_{lin}$. Thus we expect a robust nonlinear drive to the reconnection process, qualitatively similar to the one described in this paper. Now, we note that the total reconnection time is controlled by the longest of characteristic timescales associated with the various reconnection stages. When the system experiences a faster than exponential nonlinear phase, an *upper bound* to the reconnection time is given by the *linear timescale*.

Finite Larmor radius effects may further enhance the reconnection rate, When considering the $m=1$ internal kink in JET, the reconnection timescale falls in the range of 30 to $100\mu s$, in line with the observed sawtooth crash time[4,27].

Single helicity simulations of equations similar to (1-2) have been recently carried out in cylindrical geometry[38]. Numerical simulations of fluid models including some finite Larmor radius effects had been carried out earlier by Aydemir[13] and more recently by Drake et al.[39]. In all these cases, fast reconnection rates, qualitatively of the same type as discussed in the present paper, are obtained. It would be interesting to see how the phenomenology is changed by a full kinetic treatment of the electron dynamics.

To summarize, we have carried out a thorough investigation of a simple model of magnetic reconnection in collisionless of weakly collisional regimes. In spite of a number of limitations, our analysis led us to believe that the occurrence of a rapid nonlinear stage, when the system evolves faster than Sweet-Parker-Kadomtsev timescale, is a fairly general phenomenon in weakly collisional systems characterized by large values of the Δ' parameter.

ACKNOWLEDGMENTS.

The authors acknowledge stimulating discussions with J. Drake, F. Pegoraro, J. B. Taylor, F. Waelbroeck, J. Wesson and L. Zakharov.

References.

[1] S. von Goeler, W. Stodiek and N. Sauthoff, Phys. Rev. Lett. **33**, 1201 (1974).

[2] A.W.Edwards et al, Phys. Rev. Lett. **57**, 210 (1986).

[3] V.M.Vasyliunas, Rev. Geophs. Space Phys. **13**, 303 (1975).

[4] F.Porcelli, Phys. Rev. Lett. **66**, 425 (1991).

[5] H.L.Berk, S.M.Mahajan and Y.Z.Zhang, Phys.Fluids **B3**, 351 (1991).

[6] B.Coppi and P.Detragiache, Phys. Lett. **A168**, 59 (1992).

[7] L.E.Zakharov and B.Rogers, Phys. Fluids **B4**, 3285 (1992).

[8] J.Wesson, Nuclear Fusion **30**, 2545 (1990).

[9] P.A.Sweet, in *Electromagnetic Phenomena in Cosmic Physics*, ed. by B.Lehnert (Cambridge University Press, 1958), p. 123.

[10] E.N.Parker, J. Geophys. Research **62**, 509 (1957).

[11] L.Zakharov, B.Rogers and S.Migliuolo, *Phys. Fluids B* **5**, 2498 (1993).

[12] J.F.Drake and R.G.Kleva, Phys. Rev. Lett. **66**, 1458 (1991).

[13] A. Y. Aydemir, Phys. Fluids **B4**, 3469 (1992).

[14] X. Wang and A. Bhattacharjee, Physical Review Letters **70**, 1627 (1993).

[15] M. Ottaviani and F. Porcelli, Phys. Rev. Lett. **71**, 3802 (1993).

[16] F. Pegoraro and T. J. Schep, Plasma Physics and Contr. Fusion **28**, 647 (1986).

[17] T. J. Schep, F. Pegoraro and B. N. Kushinov, Phys. of Plasmas **1**, 2843 (1994).

[18] H. P. Furth, J. Killeen and M. N. Rosenbluth, Phys. Fluids **6**, 459 (1963).

[19] B. Coppi, R. Galvao, R. Pellat, M. N. Rosenbluth and P. H. Rutherford, Sov. J. Plasma Phys. **2**, 1638 (1975).

[20] B. Coppi, Phys. Lett. **11**, 226 (1964).

[21] B. Basu and B. Coppi, Phys. Fluids **24**, 465 (1981).

[22] P. H. Rutherford, Phys. Fluids **16**, 1903 (1973).

[23] F. Pegoraro, F. Porcelli and T. J. Schep, Phys. Fluids **B1**, 364 (1989).

[24] S. Migliuolo, F. Pegoraro and F. Porcelli, Phys. Fluids **B3**, 1938 (1991).

[25] R. D. Hazeltine and H. R. Strauss, Phys. Fluids **21**, 1007 (1978).

[26] J. F. Drake, Phys. Fluids **21**, 1777 (1978).

[27] T. M. Antonsen and B. Coppi, Phys Rev. Lett. **A81**, 335 (1981).

[28] A. Y. Aydemir, Phys. Fluids **B3**, 3025 (1991).

[29] F.Porcelli, in *Theory of Fusion Plasmas*, proceeding of the Joint Varenna-Lausanne International Workshop, Varenna (1992), E. Sindoni Ed., p. 161.

[30] F. M. Levinton et al., Physical Review Letters **72**, 2895 (1994).

[31] R. Kraichnan, J. Fluid Mech. **67**, 155 (1975).

[32] H. A. Rose and P. L. Sulem, J. de Physique **39**, 441 (1978).

[33] J. B. Taylor, private communication (1994).

[34] S.A.Orszag and G.S.Patterson, Phys. Rev. Lett. **28**, 76 (1972).

[35] B.B.Kadomtsev, Fiz. Plasmy **1**, 710 (1975) [Sov. J. Plasma Phys. **1**, 389 (1975)]

[36] M. Ottaviani and F. Porcelli, Proceedings of the 21st European Physical Society Conference on Controlled Fusion and Plasma Physics, Montpellier (1994), Vol. 18B, part II, p. 532.

[37] M. Ottaviani and F.Porcelli, in *Theory of Fusion Plasmas*, proceeding of the Joint Varenna-Lausanne International Workshop, Varenna (1994), E. Sindoni Ed., p. 33.

[38] D. Biskamp and J. F. Drake, Phys. Rev. Letters, **73**, 971 (1994).

[39] J. F. Drake, private communication (1994).

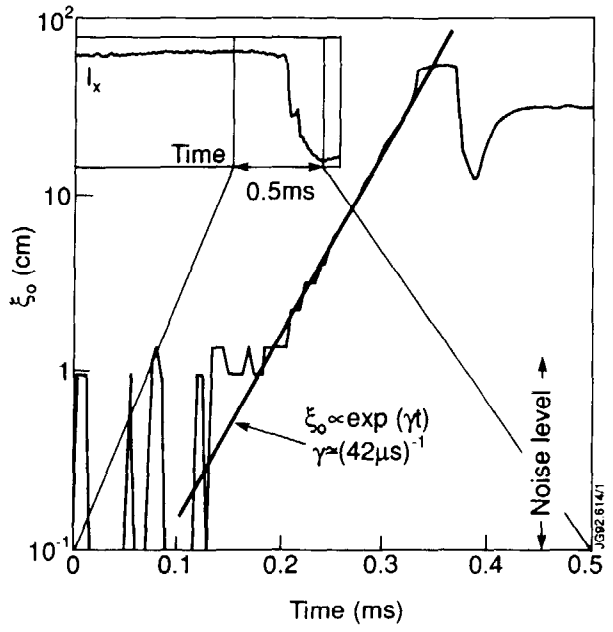

Fig. 1. Evolution of the position of the peak of the soft X-ray emissivity during a fast sawtooth crash in JET.

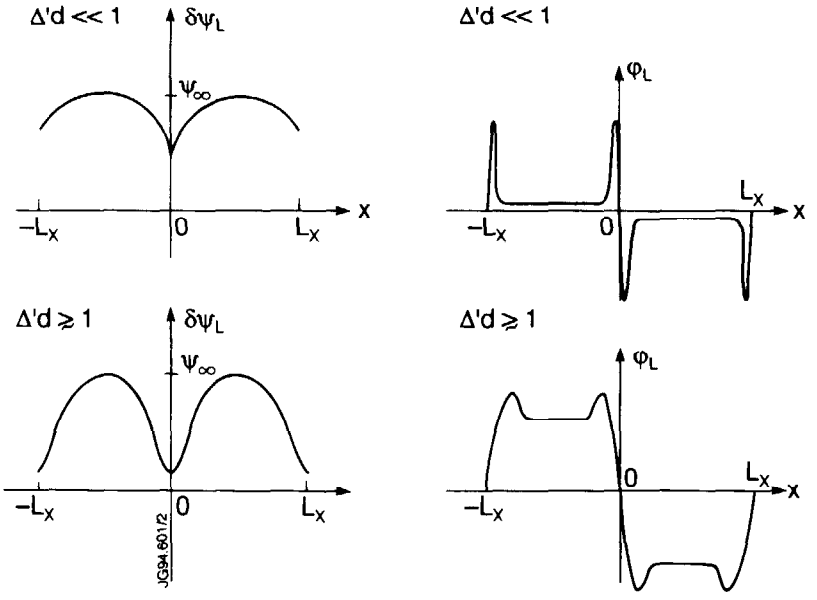

Fig. 2. Sketch of the linear mode structure of $\delta\psi_L$ and φ_L in the $\Delta' d << 1$ and $\Delta' d \geq 1$ regimes.

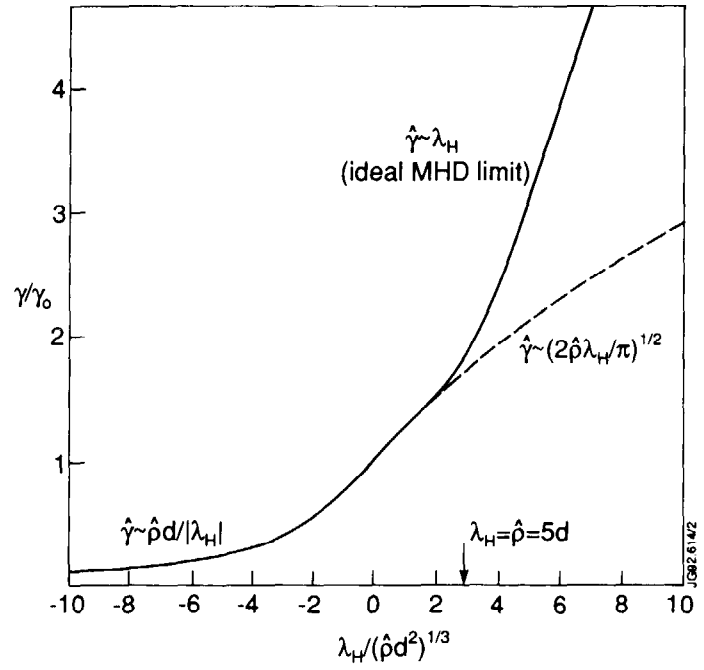

Fig. 3. Normalized growth rate γ / γ_o versus $\lambda_H / \rho^{1/3} d^{2/3}$.

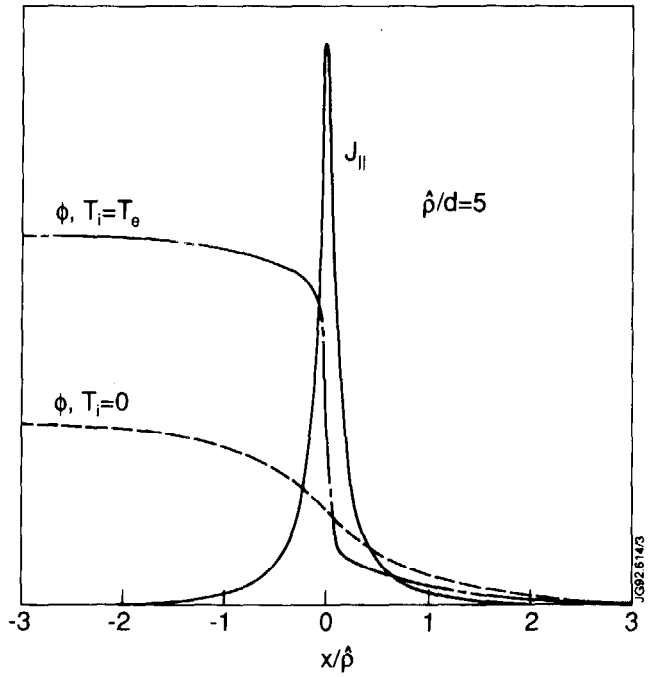

Fig. 4. Electric potential and current density eigenfunctions for two values of T_i / T_e.

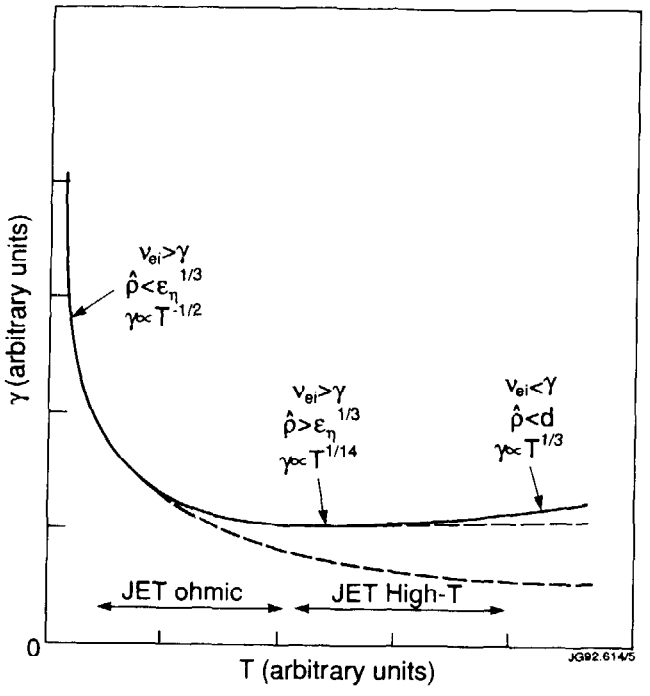

Fig. 5. Scaling of the growth rate with temperature.

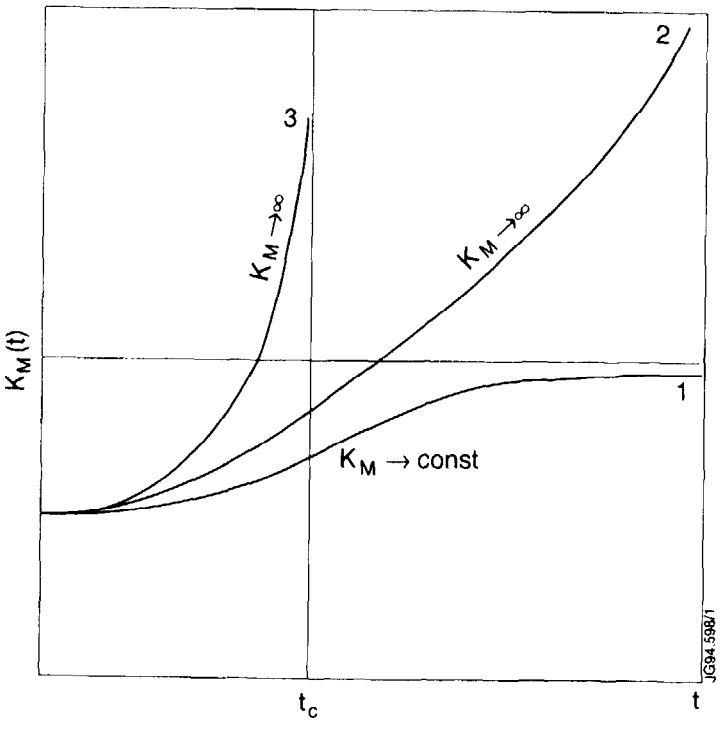

Fig. 6. Sketch of the possible behavior k_M vs time.

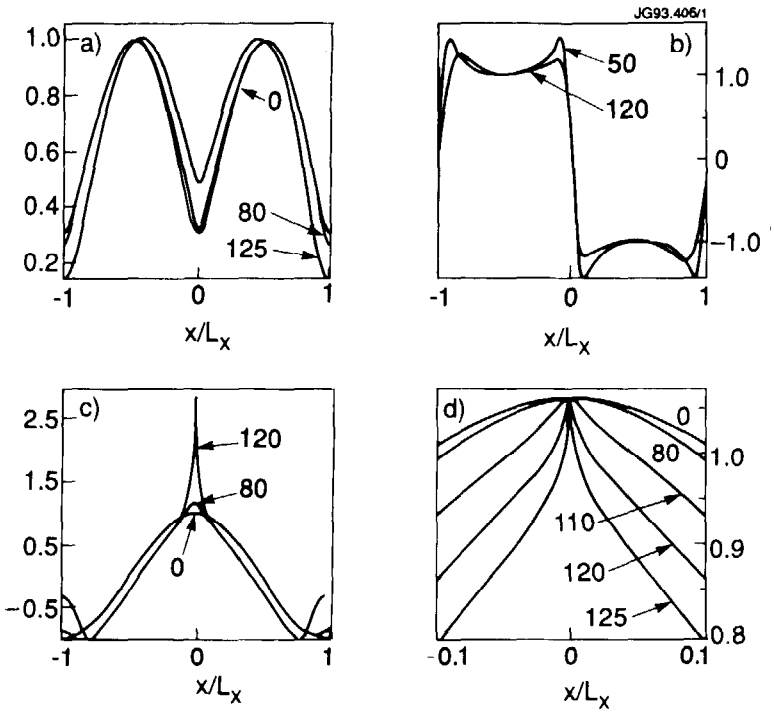

Fig. 7. Cross sections of a) $\delta\psi/(\delta\psi)_{x=L_x/2}$; b) $v_x/(v_x)_{x=-L_x/2}$; c) J; d) F versus x at $y=0$. The X-point is at $x=0$; the O-point of the second island chain is at $x=\pm L_x$. Times are indicated by the arrows.

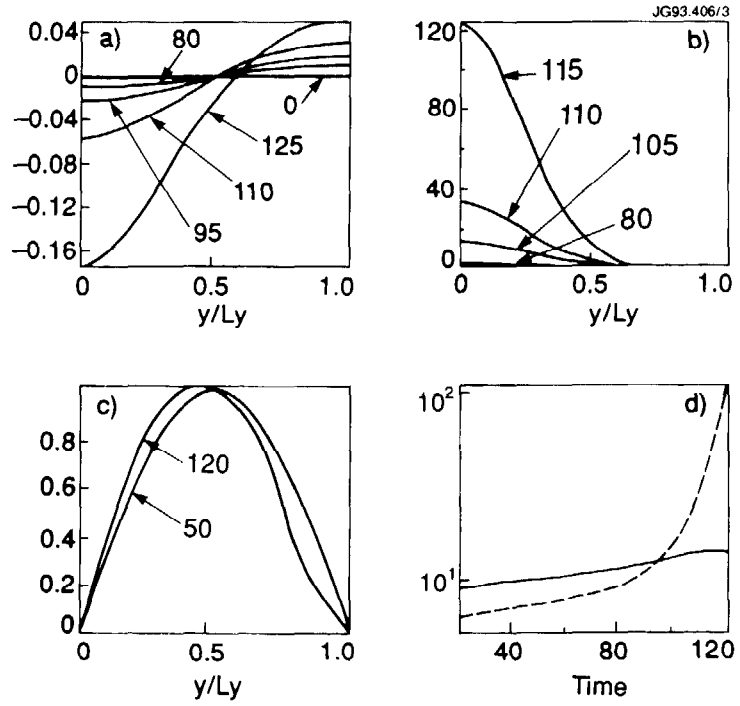

Fig. 8. Cross sections of a) $\delta\psi$; b) $\partial^2 F/\partial x^2$; c) $v_y/(v_y)_{y=L_y/2}$ versus y at $x=0$. The island's X- and O-points are at $y=0$ and $y=L_y$, respectively. Also, d) time dependence of the logarithm of the inverse scale lengths δ_φ^{-1} (solid line) and δ_J^{-1} (broken line).

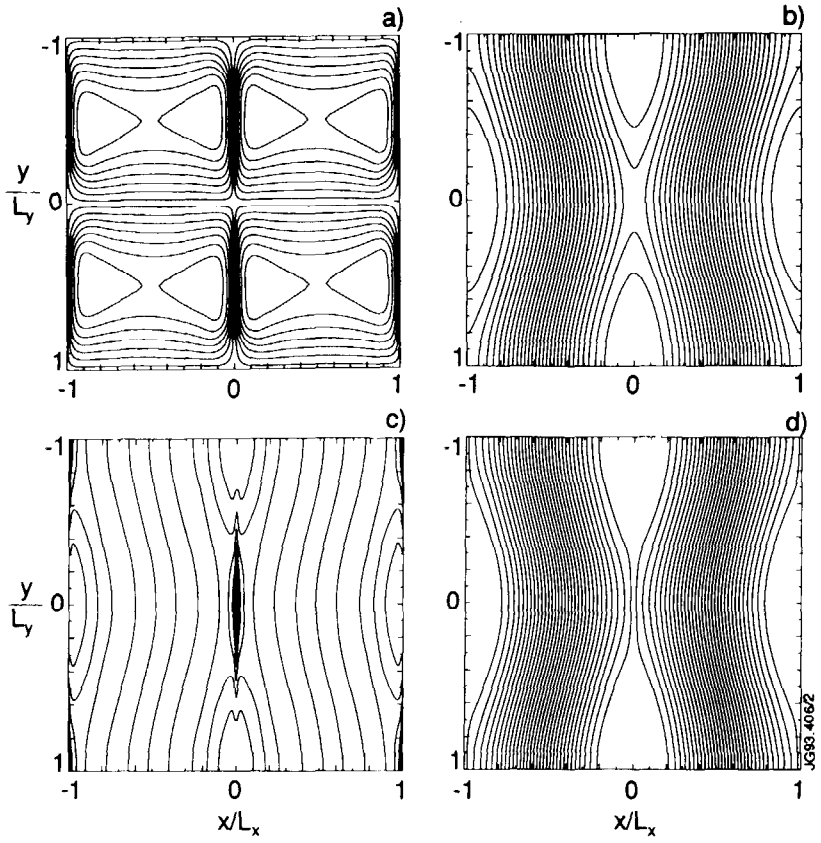

Fig. 9. Contour plots at $t=120$: a) φ; b) ψ; c) J; d) F.

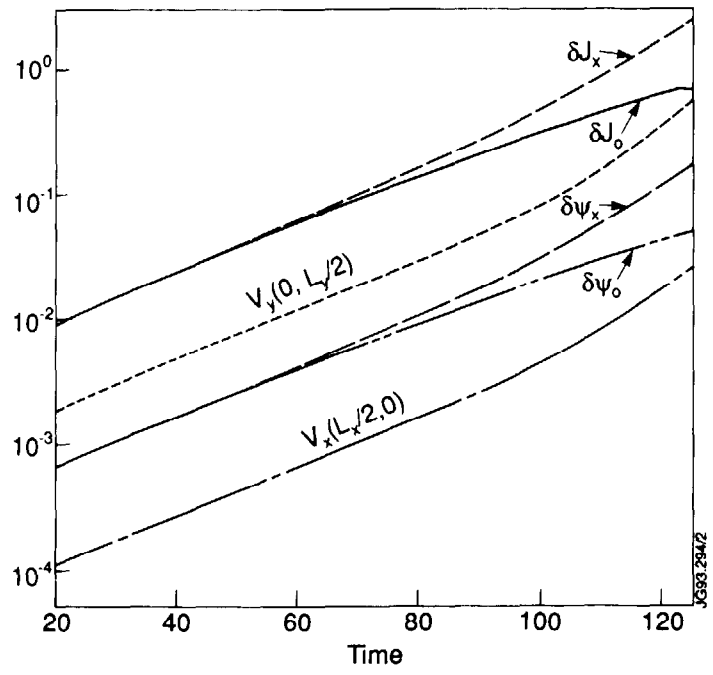

Fig. 10. Time dependence of $\delta\psi$ and δJ at the X- and O-points, of $v_x(-L_x/2,\ 0)$ and of $v_y(0,\ L_y/2)$.

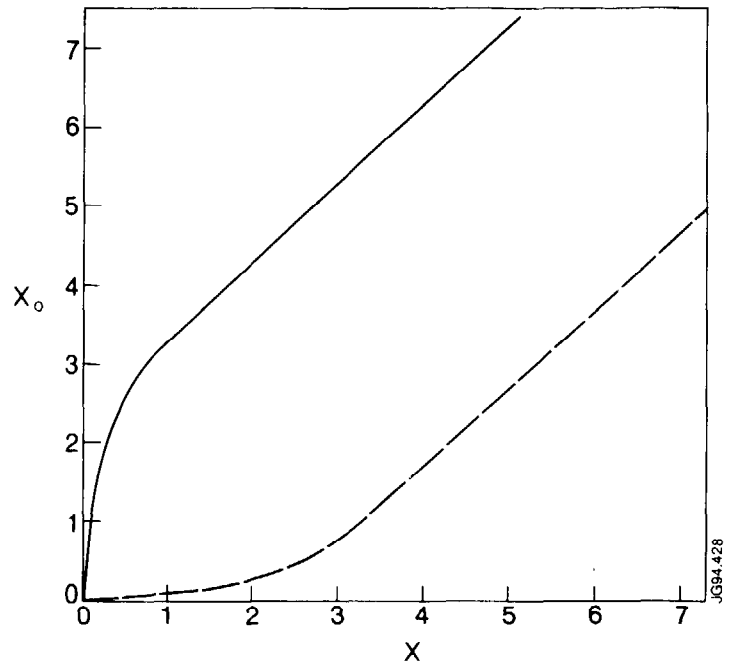

Fig. 11. Behavior of x_o vs. x at the X-point (solid line) and at the O-point (broken line). $d = 1$ and $\delta = 0.1$ in this example.

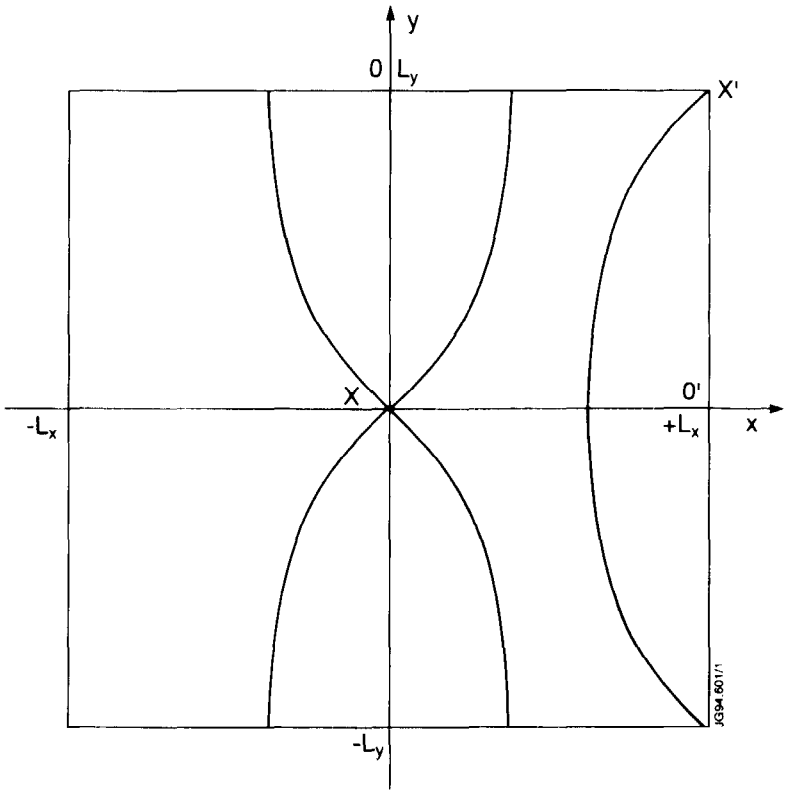

Fig. 12. Domain of integration of Eq. (39).

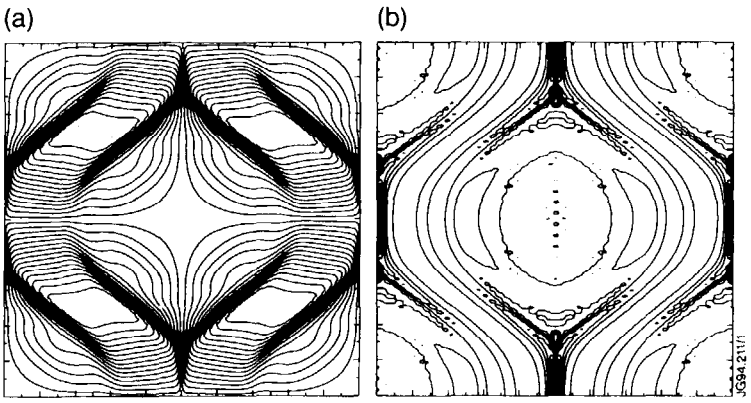

Fig. 13. Contour plots of a) the stream function φ and b) the current density J in the purely resistive case.

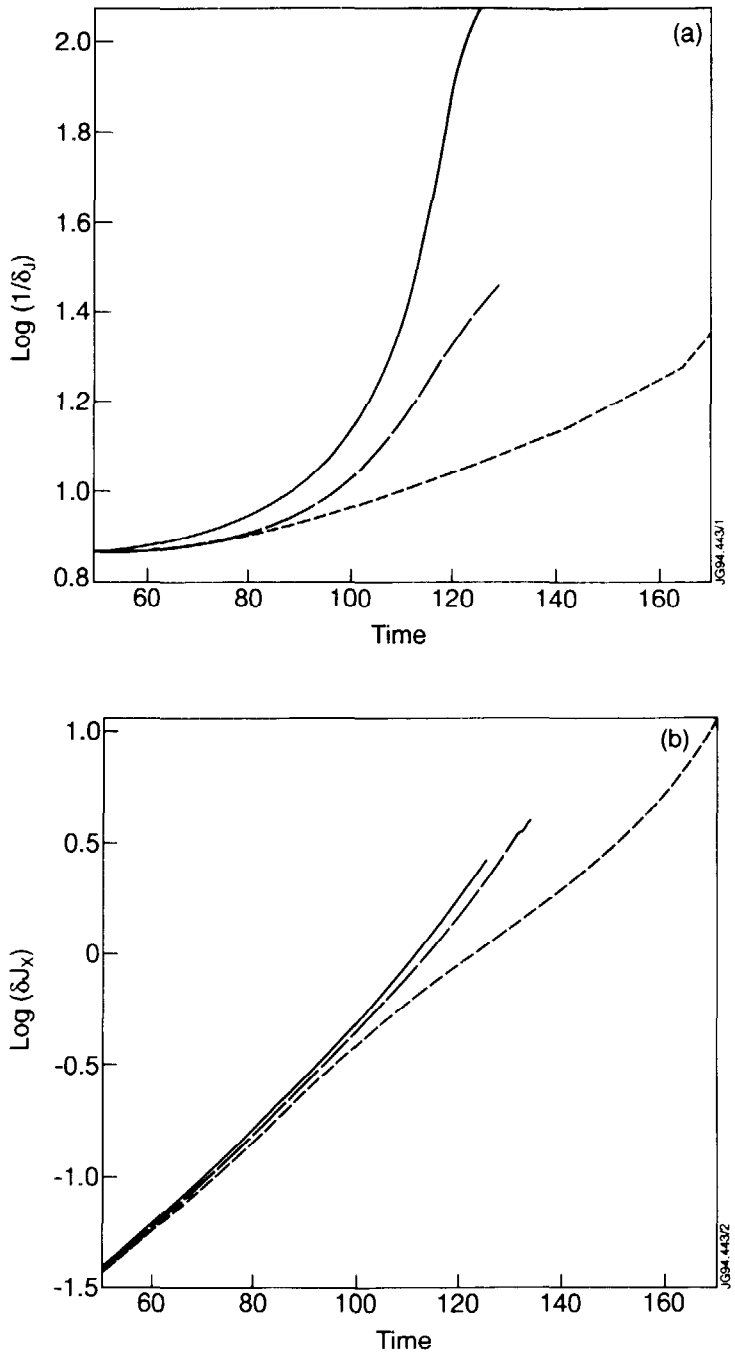

Fig. 14. Decimal logarithm of a) $\delta_J^{-1} = (\partial_x^2 \delta J)^{1/2}$ and b) δJ at the X-point vs time. Solid lines: collisionless case. Long dash: with electron viscosity $\mu_e = 6.4 \times 10^{-6}$. Short dash: pure resistive case $\eta = 3. \times 10^{-3}$.

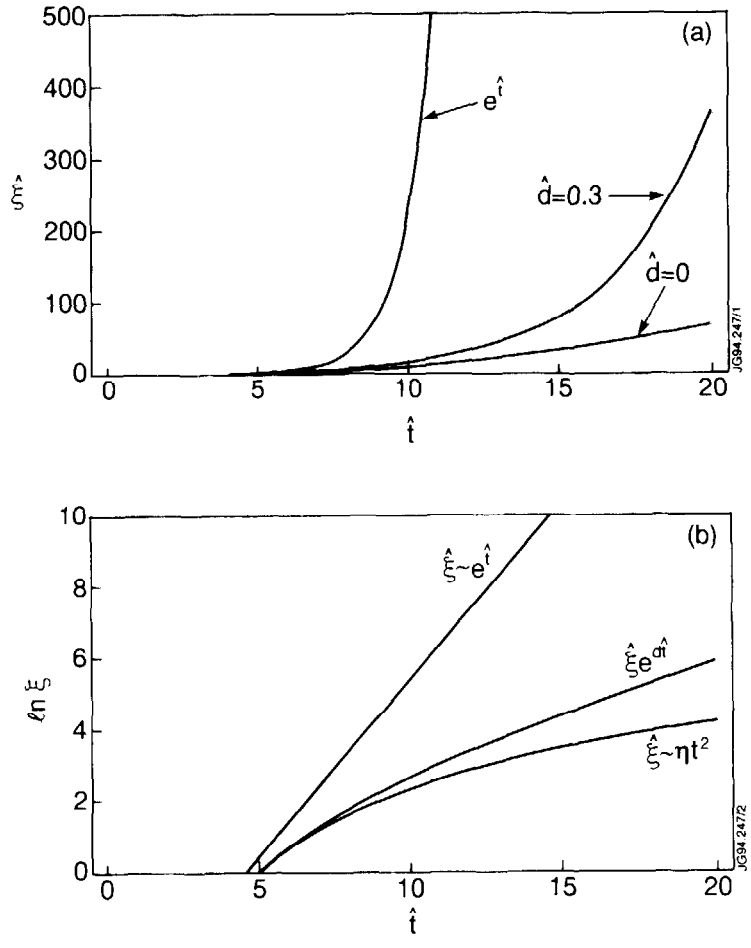

Fig. 15 Time evolution of the normalized displacement $\hat{\xi} = \lambda / \eta^{1/3}$ in the regime $\eta^{1/2} << d << \eta^{1/3}$. a) linear plot; b) semi-log plot